Seismic properties and the origin of reflectivity from a classic Paleozoic sedimentary sequence, Valley and Ridge province, southern Appalachians

NIKOLAS I. CHRISTENSEN
DANIEL L. SZYMANSKI* } *Department of Earth and Atmospheric Sciences, Purdue University, West Lafayette, Indiana 47907*

ABSTRACT

Compressional wave velocities and densities measured from samples collected along a 5-km-thick, well-exposed, thoroughly studied section of the Valley and Ridge sedimentary sequence of the southern Appalachians are used to generate a synthetic seismogram, which is compared with a reflection profile obtained directly over the stratigraphic section. The excellent agreement between the laboratory synthetic seismogram and the field data clearly demonstrate the usefulness of synthetics generated from laboratory measurements where the geology is known in detail. Seismic modeling indicates that laterally continuous, high-amplitude reflections often originate from the interior of formations, rather than at formation boundaries. High-amplitude, multicyclic reflections often arise from constructive interference of reflections from alternating shales and siltstones or limestones, whereas thick carbonate sequences are generally transparent. The clastic and carbonate rocks of this section are typical of lithologies occurring in sedimentary basins worldwide, and hence the velocity and density data of this study provide a data base for future interpretations of reflection and refraction studies in sedimentary strata of similar age. At elevated pressures, velocities range from 3.6 km/sec for propagation normal to bedding in shale to over 7.0 km/sec in dolostone. Mean densities range from 2,339 kg/m^3 for Chattanooga Shale to 2,838 kg/m^3 for Knox dolostone. The high anisotropies characteristic of shales are of major importance in modeling the reflection characteristics of sedimentary basins. Surprisingly, anisotropy is also significant in many carbonate rocks and siltstones. A useful diagram relating velocity with composition is presented for various percentages of dolostone, limestone, shale, and sandstone.

INTRODUCTION

Critical to the effective interpretation of any seismic reflection record are a thorough knowledge of the stratigraphy of an area and tight control on the seismic properties of rocks within the stratigraphic section. Stratigraphy is tied to seismic sections by converting detailed thickness information to two-way vertical traveltime using rock velocities. If the rock physical properties are well known, a synthetic reflection seismogram can be generated to aid the interpreter in tying the geology to the seismic data by matching expected and observed reflection character. The closer the known stratigraphy is located to the seismic line, the more likely it will benefit the interpretation. In frontier areas, with little or no well control, the ideal situation places a seismic line over an outcropping stratigraphic section—known in great detail—which can be projected into the seismic line.

The Thorn Hill section, located in eastern Tennessee, provides an ideal focal point for seismic interpretation in the southern Valley and Ridge. A seismic line (Tegland, 1978) passes directly over a beautifully exposed, complete, and thoroughly studied stratigraphic section (Hall and Amick, 1934; Walker, 1985). In this paper, we present detailed physical property data for a complete set of lithologies from the Thorn Hill section. Synthetic seismograms generated from the physical property data compared with the seismic profile provide valuable constraints for the interpretation of reflection sections in the southern Valley and Ridge.

Of regional significance, several small oil and gas fields produce from Ordovician and Mississippian strata in southwestern Virginia, northeast of the Thorn Hill section (Miller, 1973), but most of the southern Valley and Ridge remains untested due to structural and stratigraphic complexities, and because the discoveries to date have been small. An intriguing idea that has been speculated on for years proposes that the Valley and Ridge sedimentary sequence extends well to the southeast beneath crystalline rocks of the southern Appalachians (for example, Bryant and Reed, 1970; Hatcher, 1971, 1972). If true, this could substantially expand the potential hydrocarbon province and carry important implications for the timing and mechanics of overthrusting in the Appalachians. Factors such as metamorphism and the timing of deformational and thermal events govern the possible occurrence of hydrocarbons in any sedimentary rocks preserved beneath the Blue Ridge–Piedmont thrust (Hatcher, 1982). Metamorphism of the Valley and Ridge will affect velocities, densities, and hence the reflectivity of the sedimentary sequence. Knowledge of the reflectivity characteristics of the sedimentary section is thus essential in any assessment of the hydrocarbon potential of the southern and central Appalachian overthrust belt.

The carbonate and clastic rocks of the Thorn Hill section are typical of lithologies occurring in sedimentary basins worldwide. The excellent tie achieved between our laboratory model and the field data clearly demonstrates the usefulness of detailed surface sampling and physical property measurements for interpreting subsurface lithologies from reflection records.

*Present address: Chevron USA, Bakersfield, California 93309.

Additional material for this article (tables) may be secured free of charge by requesting Supplementary Data 9102 from the GSA Documents Secretary.

Geological Society of America Bulletin, v. 103, p. 277–289, 14 figs., 1 table, February 1991.

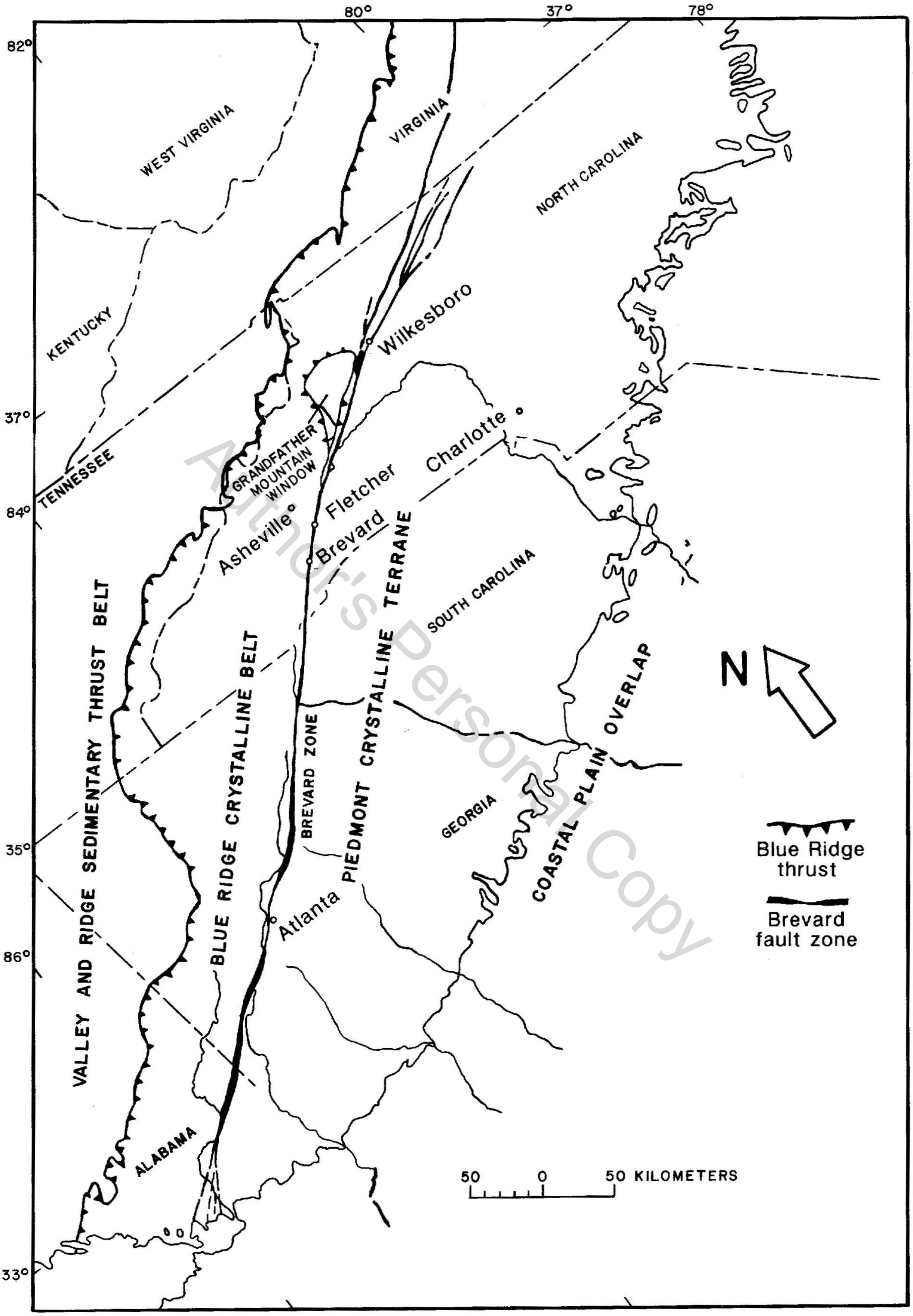

Figure 1. Map of geologic provinces of the southern Appalachians.

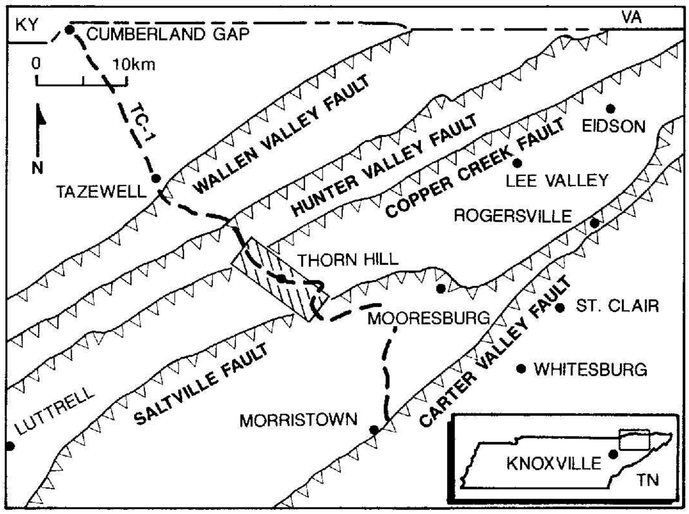

Figure 2. Simplified map of Valley and Ridge faults, Thorn Hill section location, and Line TC-1 location along U.S. Highway 25E (Tegland, 1978).

THE THORN HILL SECTION

From northwest to southeast, the southern Appalachians can be divided into four physiographic provinces: the Plateau, Valley and Ridge, Blue Ridge, and Piedmont provinces (Fig. 1). The Valley and Ridge province is dominated by linear ridges of resistant Paleozoic sedimentary rocks separated by valleys of more easily eroded units. The southern Valley and Ridge is the product of pervasive, northwest-directed Alleghanian thrust faults that repeated the Paleozoic section (Fig. 2).

The Valley and Ridge samples collected for velocity studies were obtained from exposures along a 13-km stretch of U.S. Highway 25E in eastern Tennessee (TC-1 in Fig. 2). This 3,327-m-thick, southeast-dipping section, known as the "Thorn Hill stratigraphic section," is one of the most complete and best exposed Paleozoic sections in the southern Appalachians. It starts above the Copper Creek fault in the Lower Cambrian Rome Formation and is terminated to the southeast in the Lower Mississippian Grainger Formation, which has been overthrust by the Rome along the Saltville fault. The thicknesses and ages of the major units and our sample distribution are summarized in Figure 3. The following brief discussion of lithologies and depositional environments is based on detailed descriptions of the Thorn Hill section presented in a field trip guide edited by Walker (1985). The rock descriptions and measured sections provided in the guide have proven invaluable for our collecting (see Fig. 3) and construction of the velocity column and the synthetic reflection seismograms.

The lowermost three units of the Thorn Hill section (the Rome Formation, the Conasauga Group, and the Knox Group) formed in a westward-transgressing sea. The Cambrian Rome Formation above the Copper Creek fault at this locality consists of alternating siltstone, shale, sandstone, silty dolostone, and limestone. Calcareous siltstones (samples TH-2 and TH-35), a fossiliferous limestone (TH-3), and silty limestones (TH-1 and TH-34) were collected from the Rome. Members of the overlying Conasauga Group, in ascending order, are the Pumpkin Valley Shale, Rutledge Limestone (TH-5), Rogersville Shale (with its Craig Limestone Member (TH-7)), Maryville Limestone (TH-6), Nolichucky Shale (TH-8), and Maynardville Limestone (TH-9, TH-10). The overlying Cambro-Ordovician Knox Group, one of the thickest units of the Thorn Hill section (Fig. 3), contains a preponderance of dolomite with minor limestone and quartz sandstone. In ascending order, the Knox has been subdivided into the Copper Ridge Dolomite (TH-11), Chepultepec Dolomite (TH-12), Kingsport Formation (TH-33), and Mascot Dolomite (TH-13). Deposition ceased by the end of Early Ordovician time, and a disconformity separates the Knox from the overlying depositional sequence consisting of the Lower Chickamauga Group, Middle Chickamauga Group, Moccasin Formation, Martinsburg Formation, Juniata Formation, and Clinch Sandstone (Fig. 3).

The Lower Chickamauga Group, which is divided into the Five Oaks (TH-14), Lincolnshire (TH-15), and Rockdell (TH-16) Formations, consists primarily of fossiliferous limestone formed in a shallow-water depositional environment. The Middle Ordovician Middle Chickamauga Group consists of intercalated limestone and shale formed in a carbonate-shelf environment. In ascending order, the Middle Chickamauga is subdivided into the Benbolt (TH-17), Wardell (TH-36), Bowen (TH-37), and Witten (TH-19) Formations. The overlying Moccasin Formation contains semi-fissile shale and siltstone (TH-21), fossiliferous limestone (TH-4), and argillaceous limestone (TH-20 and TH-32), originating in a tidal flat complex that covered much of the area. The Martinsburg Formation consists of a lower shale facies which is conformable with the underlying Moccasin Formation, a carbonate facies (TH-22), and an upper mixed carbonate-clastic facies (TH-23). This sequence is interpreted as having formed during an initial transgression, followed by deposition in shallower water of the mixed carbonate-clastic facies, which grade upward into the peritidal facies of the Juniata Formation. The Upper Ordovician Juniata Formation consists of red sandstone, siltstone (TH-24), silty-shale, and shale, which are commonly unfossiliferous and typically contain some carbonate. The Juniata is conformably overlain by the Lower Silurian Clinch Formation, which is subdivided into (1) the lower Hagan Shale Member, consisting of clayey siltstone and siltstone (TH-31), and (2) the upper Poor Valley Ridge Member. The Poor Valley Ridge Member consists of white, fine- to medium-grained, quartz sandstone (TH-25) with subordinate silty sandstone and siltstone deposited in a shallow-marine environment.

The third and uppermost depositional sequence of the Thorn Hill section consists of Devonian-Mississippian strata which unconformably overlie the Clinch Sandstone. The Lower Devonian Wildcat Valley Sandstone (TH-30) is overlain by Upper Devonian to Lower Mississippian Chattanooga Shale which has been divided into a lower Millboro Member consisting of black shale (TH-26), a middle Brallier Member of siltstone and silty shale (TH-29), and an upper siltstone and shale Big Stone Gap Member (TH-27). The Early Mississippian Grainger Formation, which was deposited in a shallow tidal environment, is conformable with the underlying Chattanooga Shale. It consists of a basal siltstone member, a middle silty shale and siltstone member (TH-28), and an upper sandstone member. Along Highway 25E, the Grainger is overthrust by the Lower Cambrian Rome Formation along the Saltville fault (Fig. 2).

EXPERIMENTAL TECHNIQUE AND VELOCITY DATA

The samples collected from the Thorn Hill section were selected to obtain a wide variety of lithologies as well as to give the best possible representation of the major stratigraphic units. Most samples were field oriented. To investigate seismic anisotropy, three cores with mutually perpendicular axes were drilled from each sample. The A cores were taken with the axes normal to bedding. The B cores were oriented parallel to strike with the axes in bedding planes. The C cores were oriented with the axes in the bedding planes and parallel to dip. The cores were trimmed, weighed, and measured to calculate bulk densities and jacketed with copper foil for velocity measurements as a function of pressure.

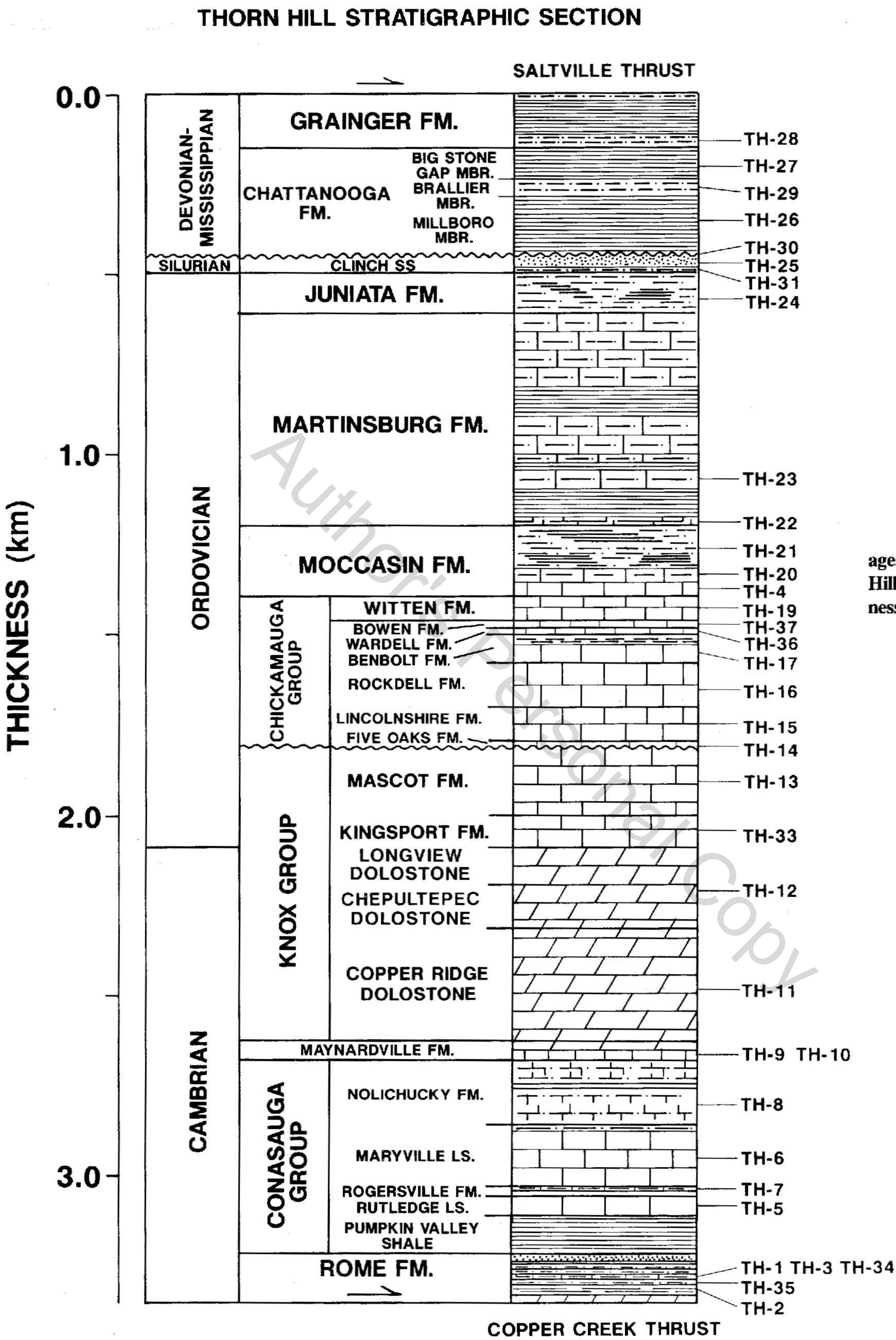

Figure 3. Thicknesses and ages of major units in the Thorn Hill section, east-central Tennessee and sample locations.

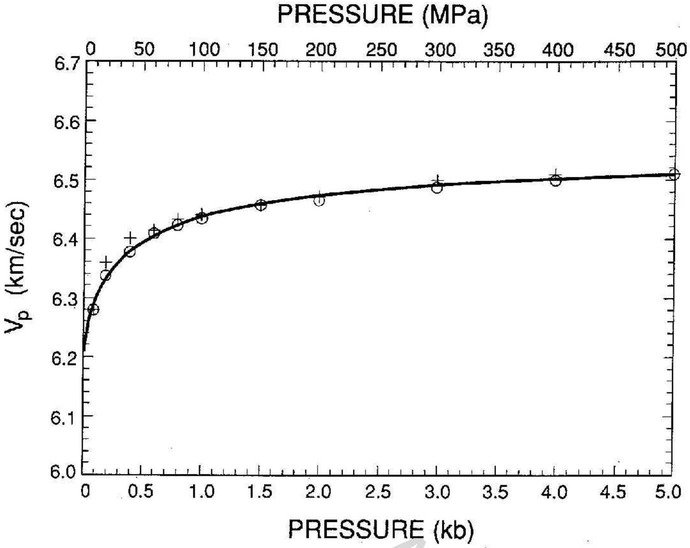

Figure 4. Compressional wave velocity as a function of pressure for sample TH-22C from the Martinsburg Formation. Plus signs indicate upgoing pressure; open circles represent downgoing pressure.

The traveltimes of compressional waves were measured using a pulse transmission technique (Birch, 1960; Christensen, 1985), and velocities were calculated from these times and the sample lengths. Natural resonant frequencies of the transducers were 1 MHz. Measurements were performed at elevated hydrostatic confining pressures using a Harwood pressure generating system with a single stage intensifier connected to a pressure vessel with an internal working space 15 cm in length and 4.5 cm in diameter. High-pressure hydraulic oil served as the pressure medium. Sample porosities ranged from 0.02% to 6.4% with an average porosity of 1.0%. The low porosities permitted measurement of velocities to 500 MPa (equivalent to depths of ~18 km) without crushing the samples. The velocities are estimated to be accurate to 1% (Christensen, 1985).

At low pressures, velocities obtained with increasing pressure frequently differ from those measured with decreasing pressure (Fig. 4), the latter usually being higher for a given pressure. Velocity, bulk density, and porosity information have been contributed to the GSA Data Repository.[1] A considerable amount of attention has been given to examining seismic anisotropy of the various rock types, which is quite significant for some samples.

SEISMIC PROPERTIES OF VALLEY AND RIDGE SEDIMENTARY ROCKS

A variety of rock types crop out along the Thorn Hill section of U.S. Highway 25E, making the section ideal for collecting Paleozoic sedimentary rocks of the southern Appalachians. The dolostones and limestones, which can be arenaceous, silty, or argillaceous, are well exposed for sampling. Likewise, road cuts of siltstones and sandstones, especially the Clinch Sandstone, which is exposed along strike for ~5 km east of Beans Gap, are fresh. Many of the argillaceous units, consisting of shale, calcareous shale, mudstone, and silty shale, are generally covered with vegetation. The fissile shales in particular were difficult to collect, resulting in a sampling bias in favor of the carbonates, but the seismic properties of all major rock types have been studied, enabling us to construct accurate velocity profiles from the detailed, measured lithologic sections of each formation.

In order of increasing velocity, the samples can be conveniently divided into subgroups consisting of (1) shale, sandstone, siltstone; (2) calcareous siltstone, argillaceous and silty limestone; (3) limestone; and (4) dolostone (Fig. 5). Notable in the figure is the fairly tight distribution of limestone velocities with a distinct peak between 6.3 and 6.6 km/sec. Scatter is related to variations in the amounts of impurities (principally clay, quartz, and dolomite) as well as anisotropy and porosity. The highest velocities were measured in the Knox Group dolostone samples. The dolostone velocities, which at elevated pressures are generally more than 7.0 km/sec (Table 1), are higher or similar to velocities measured in

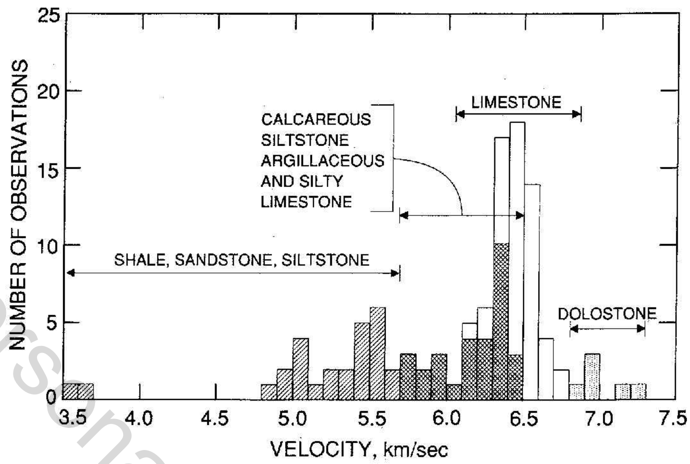

Figure 5. Velocities for various lithologies from the Thorn Hill section, measured at 200 MPa. Detailed velocity, bulk density, and porosity data are on file in the GSA Data Repository.

TABLE 1. AVERAGE ROCK VELOCITIES (km/sec) AS A FUNCTION OF PRESSURE

Pressure MPa	Shale	Sandstone	Limestone	Dolostone
	ρ = 2,350 kgm	ρ = 2,580 kgm	ρ = 2,720 kgm	ρ = 2,830 kgm
10	3.84	3.89	6.05	6.12
20	3.96	4.24	6.14	6.34
30	4.03	4.50	6.21	6.48
40	4.09	4.69	6.25	6.59
50	4.14	4.84	6.29	6.67
60	4.18	4.97	6.32	6.73
70	4.21	5.07	6.34	6.77
80	4.24	5.16	6.36	6.81
90	4.27	5.23	6.38	6.84
100	4.30	5.29	6.40	6.86
150	4.41	5.48	6.45	6.94
200	4.49	5.59	6.48	6.98
250	4.56	5.66	6.51	7.02
300	4.62	5.71	6.53	7.04
350	4.67	5.76	6.54	7.06
400	4.72	5.80	6.55	7.08
450	4.75	5.83	6.56	7.10
500	4.79	5.86	6.57	7.11

[1]To obtain free copies of these tables, request Supplementary Data 9102 from the GSA Documents Secretary.

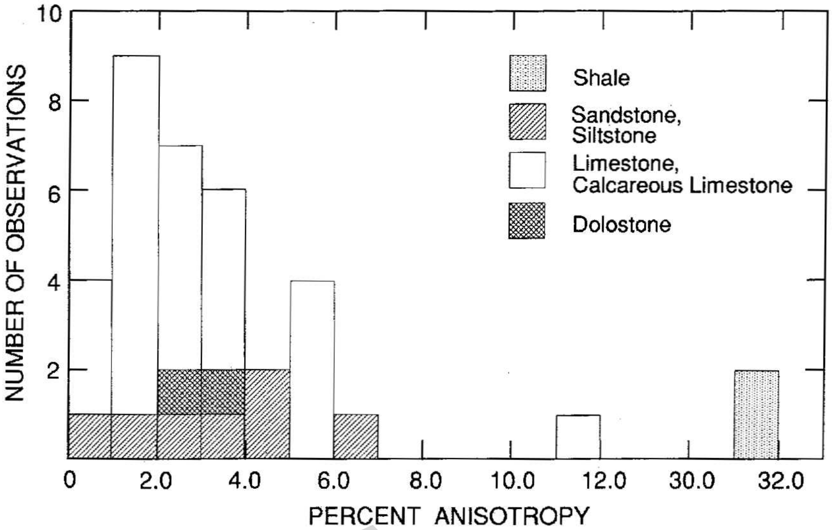

Figure 6. Velocity anisotropy (maximum velocity – minimum velocity divided by mean velocity) for various lithologies from the Thorn Hill section calculated at 200 MPa.

high-grade metamorphic rocks, including amphibolites and intermediate to mafic granulites (Christensen, 1965; Christensen and Fountain, 1975).

The shales have the lowest velocities of the Thorn Hill sedimentary rocks and display remarkable anisotropy. The two measurements of ~3.6 km/sec in Figure 5 are shale velocities for propagation normal to bedding. In the shales, bedding plane velocities at 200 MPa are as high as 5.0 km/sec, resulting in an anisotropy of 31% (Fig. 6). The sandstone and siltstone velocities vary between 4.8 and 5.7 km/sec, with argillaceous varieties generally having the lower velocities. As expected, velocities of calcareous rocks with abundant clay and silt are intermediate between limestone and siltstone (Fig. 5). Triangular diagrams illustrating variations of velocity with composition for various percentages of dolostone, limestone, shale, and sandstone (Fig. 7) may prove useful to investigators interested in reflection modeling of clastic-carbonate sequences in basins where the tie between stratigraphy and physical properties is uncertain.

For many sedimentary rocks, velocity has been shown to vary with porosity and the nature of the pore fluid. A simple, empirical, time-average equation proposed by Wyllie and others (1956),

$$\frac{1}{V} = \frac{\phi}{V_w} + \frac{1-\phi}{V_m}, \tag{1}$$

where ϕ is porosity, V_w is water velocity, and V_m is rock matrix velocity, works reasonably well for water-saturated sediments. As most porosities are less than 2%, porosity does not significantly influence velocities of the samples included in this study. An exception is the Wildcat Valley Sandstone (TH-30) with a porosity of 6.4%. The velocities and densities of the Wildcat Valley Sandstone are significantly lower than those of the lower porosity (1.9%) Clinch Sandstone.

The low-velocity shales also have the lowest bulk densities. Likewise, the fast dolomites have the highest densities of the Thorn Hill rocks. Velocities are not, however, a simple function of density (Fig. 8). The data points fall approximately into four regions in Figure 8. First, velocities of

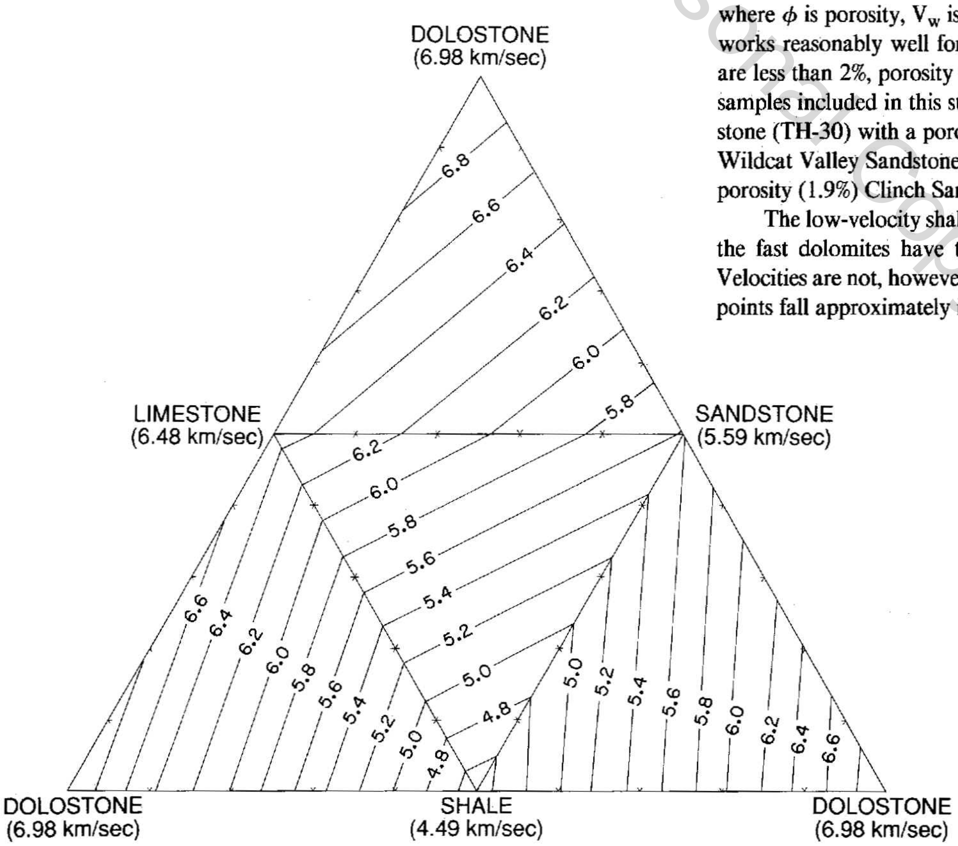

Figure 7. Average compressional wave velocities at 200 MPa for various proportions of limestone, dolostone, sandstone, and shale.

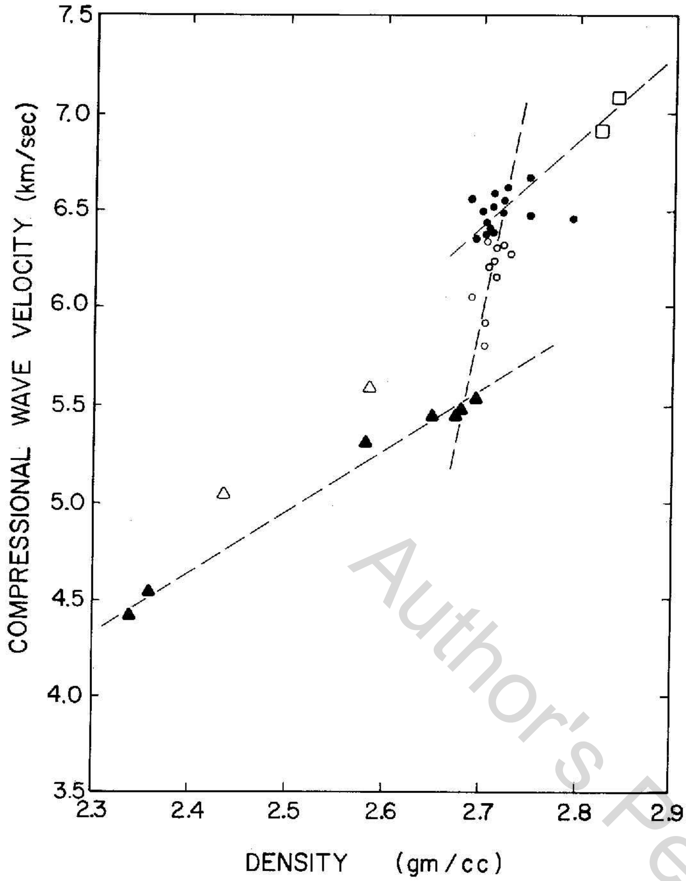

Figure 8. Average compressional wave velocity at 200 MPa in three directions versus average density for Thorn Hill rocks. Open squares = dolostones; solid dots = limestones; open circles = argillaceous and silty limestones, calcareous siltstones; solid triangles = shales and siltstones; open triangles = sandstones.

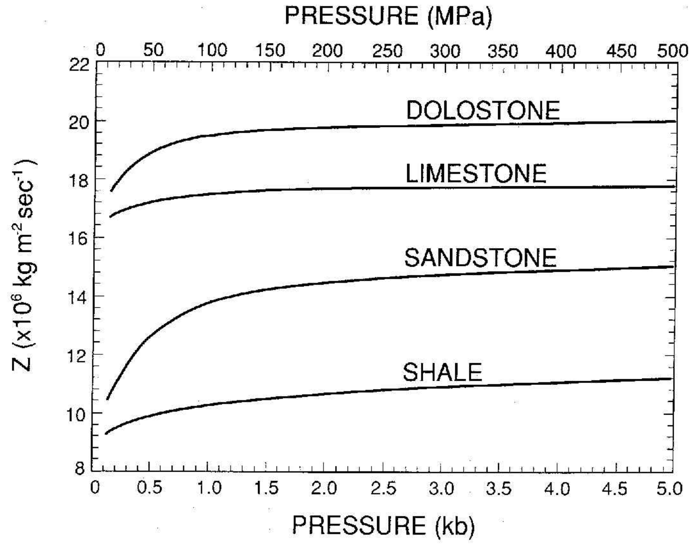

Figure 9. Acoustic impedances (Z) as a function of pressure from average velocites and densities of the Thorn Hill rocks.

the arenaceous and argillaceous rocks are observed to increase rapidly with increasing density. Second, the impure carbonates have densities (~2,700 kg/m^3) similar to limestones, but they exhibit a fairly wide range in velocity. Third, the limestones are tightly clustered around velocities of 6.5 km/sec and densities of 2,720 kg/m^3. Finally, the dolomites fall into a distinct field of high velocity and density. It is clear from Figure 8 that a simple, linear, velocity-density relation is inappropriate for these Paleozoic sedimentary rocks.

The samples that we have studied show wide variations in compressional-wave anisotropy (Fig. 6). The sandstones are virtually isotropic, whereas the shales show extreme anisotropy at all pressures. The velocity differences found for the three mutually perpendicular propagation directions may arise from preferred mineral orientation as well as variations in composition of the three cores. Similar densities of the three cores from a given specimen and high anisotropy usually indicate a preferred orientation of highly anisotropic minerals as a cause for the anisotropy (Christensen, 1965), which for shale is clay mineral orientation.

Some carbonates show anisotropies of several percent, but others are virtually isotropic (Fig. 6). Velocities of the anisotropic samples are often low, normal to the bedding. Preferred orientations of accessory clay minerals, or even calcite and dolomite, may be responsible for this anisotropy.

For a normally incident ray, the ratio of the amplitude of the reflected ray to the amplitude of the incident ray is given by

$$R = \frac{\rho_2 V_2 - \rho_1 V_1}{\rho_2 V_2 + \rho_1 V_1} = \frac{Z_2 - Z_1}{Z_2 + Z_1} \qquad (2)$$

where $\rho_1 V_1$ and $\rho_2 V_2$ are the products of density and velocity, termed acoustic impedance (Z), above and below the interface separating two lithologies, respectively. The acoustic impedance is characteristic of lithology (Fig. 9). The reflection coefficient, R, ranges from −1 to +1. If R = +1 or −1, all of the incident energy is reflected, whereas if R = 0, all of the energy is transmitted. A negative value of R corresponds to a 180° phase change in the reflected wavelet. Calculated values of reflection coefficients for various combinations of Thorn Hill rocks range from −0.4 to +0.4 (Fig. 10), with the highest magnitudes of R originating from shale-dolomite interfaces.

The high anisotropies characteristic of the shales are of considerable importance in modeling the reflection characteristics of the Valley and Ridge stratigraphic section. In Figure 10a, reflection coefficients for the interface between an overlying shale (with average acoustic impedances of TH-26 and TH-29) and various underlying sedimentary rocks are shown assuming anisotropic and isotropic shale velocities. The lower reflection coefficients for each sample were obtained using shale velocities averaged for three directions, whereas the higher reflection coefficients were obtained using velocities measured normal to the shale bedding planes (A-cores). The latter are correct reflection coefficients for normal incidence in horizontally layered strata. Similar calculations of reflection coefficients can be made for dolostone and sandstone overlying different lithologies (Figs. 10b and 10c).

Shales in contact with carbonates produce maximum-amplitude reflections with reflection coefficients between ±0.33 and ±0.41. Carbonate-sandstone and carbonate-siltstone reflection coefficients in general are quite large (±0.06 to ±0.22), with the maximum values corresponding to sandstone-dolostone interfaces. Limestone-dolostone reflections are less than ±0.05 and hence give rise to weak reflections, but simple reflections can be enhanced or destroyed by the interference of reflections from overlying and underlying interfaces.

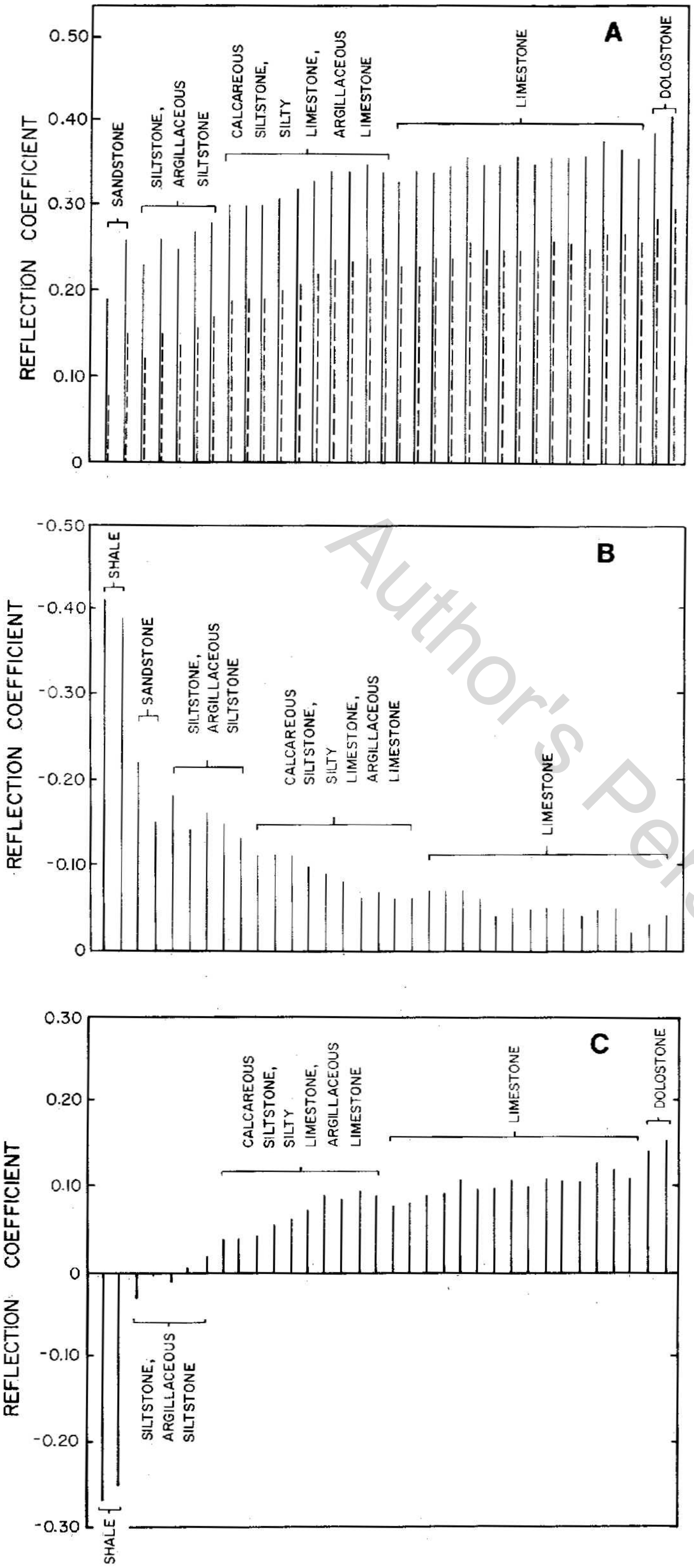

Figure 10. Reflection coefficients at 200 MPa for (A) rocks underlying shale (dashed lines assume isotropy, and solid lines assume anisotropy); (B) rocks underlying dolostone; and (C) rocks underlying sandstone.

SEISMIC REFLECTION INVESTIGATIONS IN THE SOUTHERN VALLEY AND RIDGE

Recognition of major thrust faults in the Paleozoic strata of the southern Valley and Ridge by geologists led to debates over the extent of basement involvement in the deformation. The inability to settle this question, as well as oil industry interest in hydrocarbon accumulations (for example, Mitra, 1988), attracted seismic reflection investigators to the area.

The results of the first published reflection work in the southern Valley and Ridge were described by Harris (1976). This 32-km-long Vibroseis line extended from Kingston to Dixie Lee Junction, Tennessee, just southwest of Knoxville (Fig. 2). Harris recognized distinctive seismic signatures for the Rome Formation, Conasauga Group, and Knox Group. Using these patterns and limited well data (Harris, 1970; Miller, 1973) as a guideline, Harris noted that major reflectors in the Rome could be traced from outcrop as they dip to the southeast and gradually flatten and merge into a zone of highly reflective, nearly horizontal layers that overlie interpreted basement. Harris proposed a root zone for all faults residing in these reflectors very close to the contact between basement and the overlying Paleozoic section. The basement itself is characterized by discontinuous reflections.

Tegland (1978) summarized a regional seismic investigation in eastern Tennessee. Lines K-1 South and TC-1 extend 64 km along U.S. 25 from Cumberland Gap to Morristown. Line TC-2 runs ~96 km along TN 70 from Powell Mountain at the Virginia border to the Hot Springs window at the North Carolina border (Fig. 2). The three lines cover most of the Valley and Ridge in eastern Tennessee from the Cumberland Plateau to the leading edge of the crystalline Blue Ridge allochthon. Of major significance to this study, line TC-1 passes directly over the Thorn Hill section.

A significant feature of Tegland's profiles is the association of the shaley units with the thrust faults, especially the Cambrian Rome Formation and Conasauga Group in the lower thrusts and the Lower Silurian Rockwood Formation and Devonian Chattanooga Shale in the upper thrusts. Reflections are multicyclic, high-amplitude, and strongest where the preserved glide unit is thickest. These reflections apparently arise from lithologic variations within the Rome Formation and Conasauga Group, which are known to contain interbedded carbonate and shale, rather than from simple fault contacts. Indeed, where faults cut through competent formations, or preserve only a thin section of the incompetent glide unit, or travel within shales that are void of interbedded carbonates, the reflections are monocyclic, low amplitude, and difficult to trace. The success of accurately locating a thrust fault is commonly dependent on the preservation of an appropriate thickness of a pre-existing, inherently reflective glide unit. This is amply demonstrated in the seismic data interpreted by Mitra (1988). The continuity of individual reflectors within the Rome and Conasauga over distances of several miles normal to strike indicates a remarkable geologic continuity to the individual beds. Milici and others (1979) added that the seismic lines reported on by Tegland revealed numerous west-to-east facies changes, which are manifested as lateral changes in reflection character. The interpretation of Milici and others also suggested that Cambro-Ordovician strata with a total thickness of 6.0 km project beneath the crystalline Blue Ridge thrust sheet, which is 0.9 to 1.2 km thick at its leading edge. Subsequent reflection studies by Clark and others (1979), Cook and others (1979, 1983), and Harris and others (1981) in the crystalline Blue Ridge and Piedmont proposed that the Paleozoic strata continue far eastward beneath the Blue Ridge and Piedmont allochthons. Interpretations of recent high-quality seismic reflection data by Coruh and

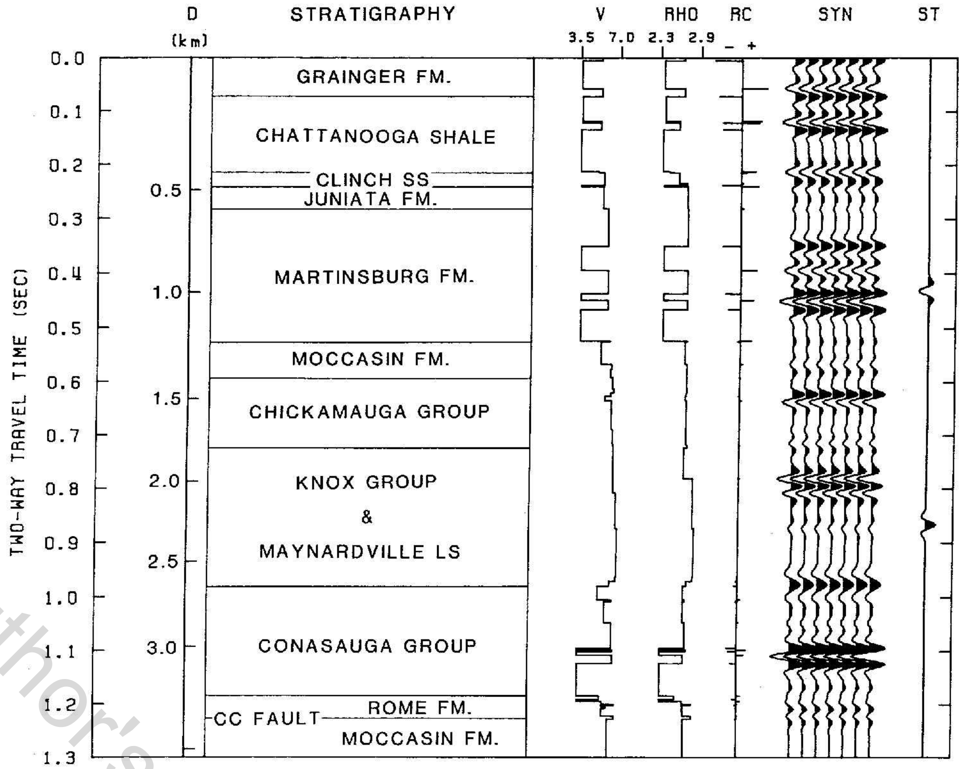

Figure 11. Vertical incidence synthetic seismogram for the stratigraphic column exposed in the Thorn Hill section (see text).

others (1987) and Hatcher and others (1987) place sedimentary platform rocks as far southeast as the Inner Piedmont province.

In summary, reflection work leaves little doubt as to the thin-skinned nature of Valley and Ridge faults, showing minimal basement involvement. Furthermore, this work demonstrates the utility of seismic reflection records in recognizing facies changes and in determining the subsurface position and interaction of faults, including possible hydrocarbon traps. Critical to these and any seismic reflection interpretation is the correct identification of seismic reflection signatures of the known stratigraphy. The approach taken by Harris (1976), Tegland (1978), and Milici and others (1979) was the use of "seismic type sections" derived from reflection records recorded over areas of well-known stratigraphy. A more exact and useful approach is to tie the known stratigraphy to the seismic sections using synthetic reflection seismograms. To generate meaningful synthetics, both the stratigraphy and rock physical properties must be known in great detail, as they are for the Thorn Hill section.

REFLECTIVITY OF THE THORN HILL SECTION

Synthetic reflection modeling of actual geologic sections can aid in understanding crustal reflectivity. Using the laboratory velocity and density data and measured thicknesses of the lithologic units, a time series containing reflection coefficient information was computed for the Thorn Hill section. This series was convolved with a zero-phase, 25-Hz, three-extrema wavelet to produce the synthetic seismogram modeled in Figure 11. 25 Hz represents a frequency commonly exploited in crustal surveys. For positive reflection coefficients, reflections appear as excursions to the left, bordered by two shaded, symmetric, lower amplitude peaks. Noise and multiple reflections are not shown. Transmission losses are accounted for, but the record has been gained using a 260-msec window to better match the field data.

The vertical axis of Figure 11 is total two-way traveltime, which is ~1.25 sec for the Thorn Hill section. The one-way depth scale, in 0.5-km intervals, is labeled "D". To the right is the Thorn Hill stratigraphic section. The velocity (V) and density (RHO) columns show the velocity and density distributions used to calculate the synthetic trace. Velocities measured at 200 MPa, corresponding to the pressure regime where most of the microcracks in the sample have closed, were used in the model. The reflection coefficient series (RC) depicts increases in acoustic impedances as spikes to the right, and decreases as spikes to the left. The effects of transmission losses can be seen as these spikes generally become smaller

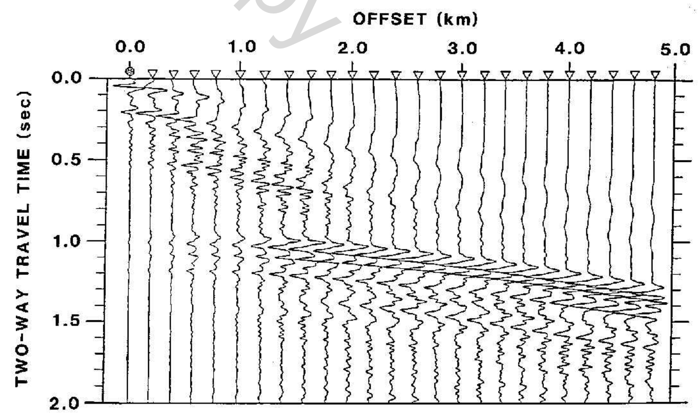

Figure 12. Single-shot synthetic reflection gather for the Thorn Hill section, showing primary- and multiple-reflection events. The traces would be NMO-corrected and stacked to produce a single trace on a CMP-gather section.

with depth. The resulting synthetic seismogram (SYN) is repeated seven times to simulate a segment of a zero-offset, two-dimensional seismic record. An ungained standard trace, corresponding to a three-layer model consisting of +0.1 and −0.1 reflection coefficient interfaces, is shown for comparison.

A synthetic, single-shot, reflection gather—uncorrected for normal moveout (NMO)—was calculated using a finite-element algorithm (Fig. 12). The model shows both primary and multiple reflections arising from a 25-Hz wavelet propagating through the Thorn Hill section. If this represented an actual single-shot gather, the traces would be NMO-corrected and stacked. Most of the multiples are attenuated in the stacking process. The result is a stack similar to the simpler one-dimensional synthetic seismogram shown in Figure 11.

Because the velocity-density-thickness model used to generate Figure 11 is known very precisely, much can be said about the origin of the reflections seen in this record. The seismogram is characterized by three highly reflective zones, separated by zones of relative acoustic transparency. The uppermost zone of high-amplitude, multicyclic reflections arises from the alternating siltstone and shale of the Mississippian-Devonian Grainger and Devonian Chattanooga Shale. Amplitudes are enhanced by constructive interference of reflections from the top and base of some of these members. The 137-m-thick Millboro Member shale, forming the base of the Chattanooga Shale, appears as a transparent zone starting at 0.135 sec two-way time, but the top of the underlying Lower Silurian Clinch Sandstone (and thin Wildcat Valley Sandstone) is marked by a strong trough. The argillaceous siltstone of the Juniata Formation and the silty limestone at the top of the Martinsburg Formation are modestly reflective. Alternating shale and silty limestone in the interior of the Martinsburg Formation produce a series of bright reflections from 0.35 to 0.48 sec.

The largely carbonate Moccasin Formation, Chickamauga Group, and Knox Group create a seismically dim zone from about 0.5 to 0.95 sec. Applying gain has amplified the events at 1.5 sec and 2.0 sec; the true amplitudes are almost nil. Reflections become abundant again with the Nolichucky Shale at the top of the Conasauga Group (0.98 sec). A very obvious high-amplitude event correlates with the alternating shale and limestone of the Rogersville Shale and Rutledge Limestone within the Conasauga Group. The Rome Formation is characterized by low-amplitude reflections, due in part to destructive interference of internal reflections, but lateral facies changes may cause the Rome Formation to be more reflective elsewhere, particularly toward the west. The Copper Creek thrust, which places the Rome on Moccasin Formation carbonates, barely registers as a seismic event. Particularly in the Cambrian and Ordovician section, distinguishable reflections are rarely associated with the tops of major sequences, but rather arise from numerous vertical facies changes interior to the sequences. This fact, coupled with lateral facies variations and structural complexity, will make seismic stratigraphy difficult in this area. The interpreter may have to rely on picking key marker beds rather than unconformity surfaces.

The synthetic seismogram can be compared to a seismic panel derived from Line TC-1 across the Thorn Hill area (Fig. 13). The similarity in character between synthetic and field data is obvious. The favorable tie permits the known geology of the synthetic to be carried to the section. On the field record, the reflectivity of the Mississippian-Devonian section is not evident because it is at or near the surface, where the record is plagued by low fold and statics busts. Tying especially well are the reflectors internal to the Martinsburg Formation and Conasauga Group.

On the left side of the field data, there is an interpretation presented by Tegland (1978). Tegland converted the seismic sections from time to depth so that he could use stratigraphic thicknesses measured at the surface to aid his interpretation. He found time-to-depth conversion very difficult in the absence of reliable velocity information, and finally settled on an exponential velocity-depth relationship. Tegland's formation boundaries approximately agree with the results of our modeling, with a few notable exceptions. Much of what Tegland included in the Silurian actually belongs to the underlying Ordovician Juniata Formation. Tegland interpreted the high-amplitude reflectors internal to the Martinsburg Formation and Conasauga Group to mark the top of the underlying formations, thereby substantially underestimating the thickness of these reflective units. This demonstrates a common pitfall in seismic interpretation of assuming that high-amplitude, continuous reflectors represent time stratigraphic surfaces rather than laterally persistent lithofacies. It is essential to tie the geology to the section, in as many locations as possible. An interpretation by Milici and others (1979) correctly placed the high-amplitude reflectors *within* the Conasauga Group, but their interpretation of the overlying units in the Thorn Hill area differs significantly from the above interpretation.

The true stratigraphic thicknesses of the formations comprising the Thorn Hill section may differ in the subsurface from measured outcrop thicknesses. For instance, this could occur by lateral variations both along strike and downdip in thicknesses of the formations, or by facies changes. Furthermore, although the Thorn Hill section is relatively undisturbed structurally, internal faulting could repeat or cut out portions of the section; furthermore, accurate true dip determinations are essential for obtaining true thicknesses from exposures oblique to dip, especially when estimating thicknesses of poorly exposed lithologies. Of course, it is possible to adjust the model layer thicknesses to improve the synthetic tie (Fig. 14). Although subject to the ambiguity inherent in geophysical inversion schemes, iterating layer thicknesses to improve the tie can provide insight into lateral variations in subsurface geology, particularly when starting with the constraint of known surface geology.

Seismic modeling illustrates how thorough knowledge of the stratigraphy and physical properties of well-exposed sections can provide a "Rosetta stone" for interpreting seismic records, but areas with numerous facies changes and structural complexities will require as many such Rosetta stones as can be accurately modeled.

SUMMARY AND CONCLUSIONS

The focus of this study has been twofold: first, to present detailed velocity and density information for a wide variety of sedimentary rock types from the Valley and Ridge province of the southern Appalachians; and second, to model the reflectivity of a well-studied stratigraphic section and compare the generated synthetic with the field record. Principal conclusions are as follows.

1. Compressional wave velocities at 200 MPa range from a low of 3.5 km/sec for propagation normal to bedding in shale to a high of 7.2 km/sec parallel to bedding in dolostone. Velocities in limestone generally fall between 6.3 and 6.6 km/sec. Sandstone and siltstone velocities vary from 4.8 to 5.7 km/sec at 200 MPa.

2. Velocities of Paleozoic sedimentary rocks are not a simple linear function of density, but they correlate well with mineralogy.

3. Anisotropy in shales, which approaches 30% at 200 MPa, significantly increases reflectivity. Anisotropy is also relatively high in some carbonate rocks and siltstones.

4. Reflection coefficients within the Paleozoic section can range from −0.4 to +0.4, with the highest magnitudes originating from shale-dolomite interfaces.

5. Master triangular diagrams, showing the effects of lithologic impurities on the velocity of pure end members, can assist seismic interpreters modeling known stratigraphic sections in basins where physical property measurements are unavailable. Porosity effects can be taken into account using the Wyllie equation or other appropriate relations.

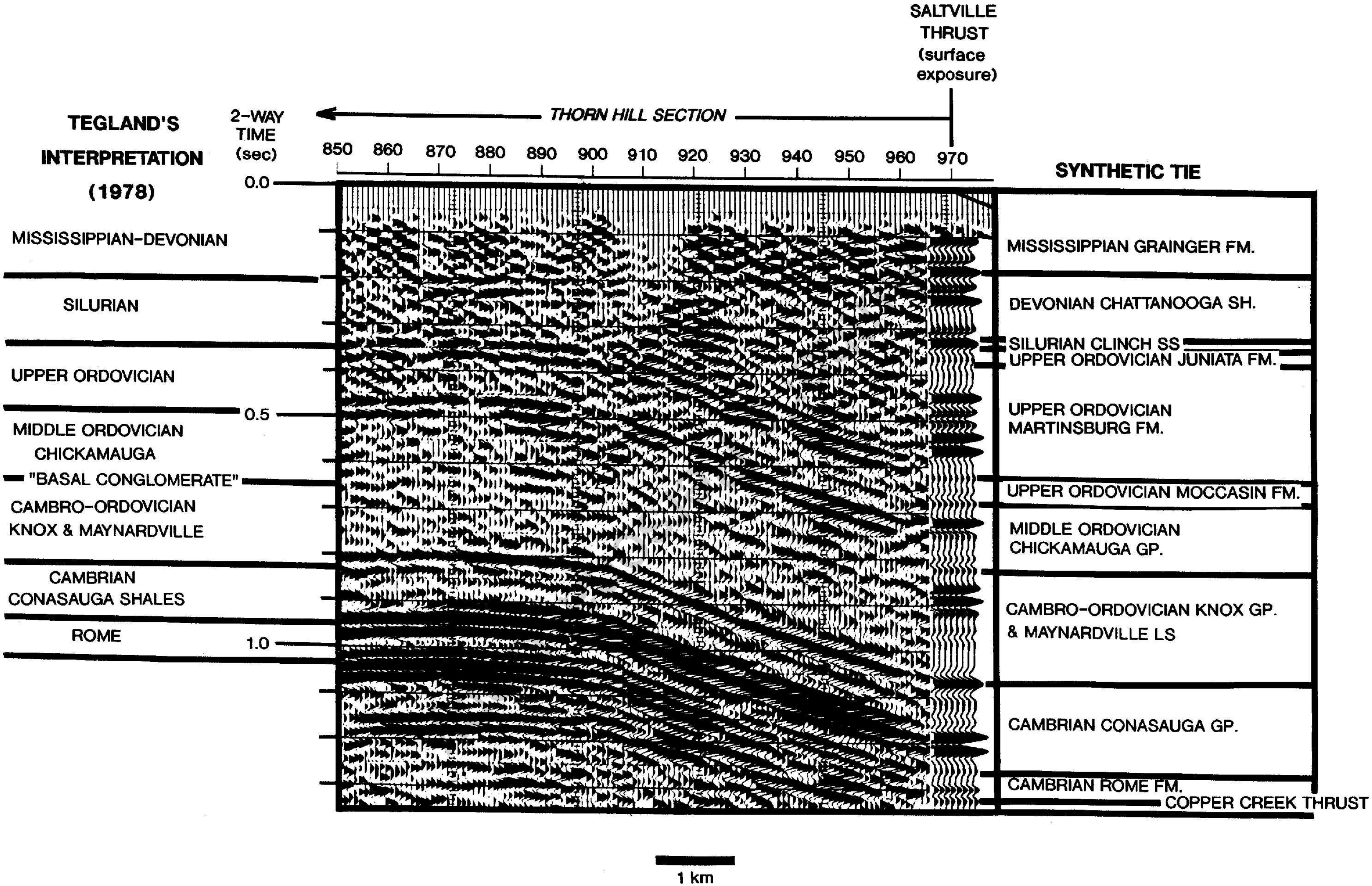

Figure 13. Tie between Thorn Hill stratigraphic section and seismic line TC-1, based on velocity and density measurements. The Thorn Hill section is exposed at the surface from shotpoint 950 northward. Tegland's (1978) interpretation is shown on left. SV = surface trace of Saltville thrust. CC = subsurface position of Copper Creek thrust.

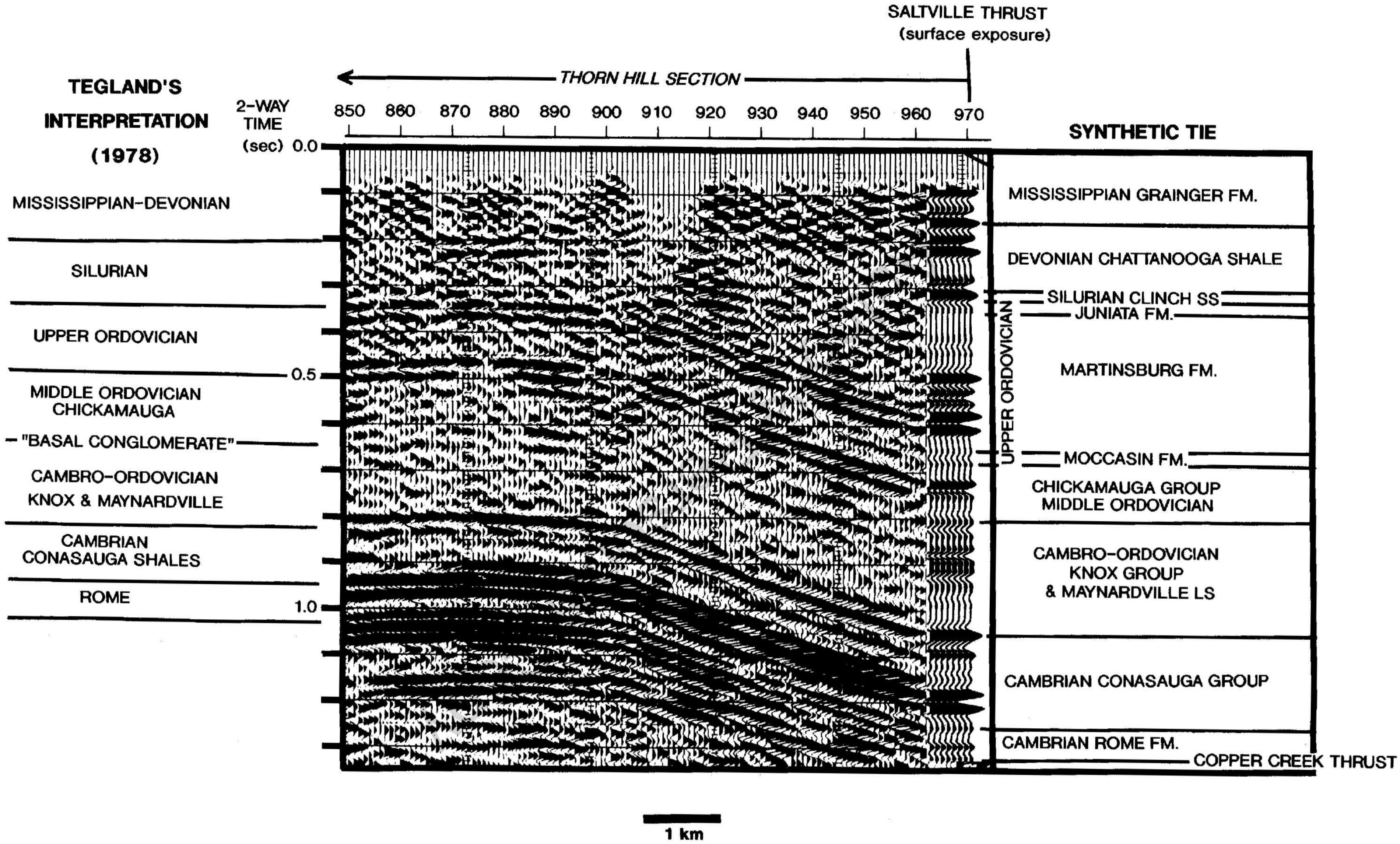

Figure 14. Improved synthetic tie between Thorn Hill section and seismic line TC-1 resulting from subtle adjusted model layer thicknesses (compare with Fig. 13). In this model, the Upper Martinsburg carbonate, Juniata Formation, Kingsport Formation, and Nolichucky Formation are assumed to be thicker than surface outcrop measurements. The Lower Martinsburg shale, Chepultepec dolostone, and Copper Ridge dolostone are allowed to thin, and so the total Thorn Hill section thickness is preserved.

6. Interference between reflections arising from the tops and bases of closely spaced beds can significantly enhance or destroy the individual reflection events.

7. Laterally continuous, high-amplitude reflections often characterize the interior of formations, rather than formation boundaries. In this case, the reflectors represent laterally persistent facies and may not indicate time-stratigraphic boundaries (that is, unconformities). In order to apply seismic stratigraphy to interpretation of such complicated areas, the geology must be tied to the sections in as many locations as possible.

8. Accurate physical property information and detailed stratigraphic columns are essential for working seismic data in areas with scarce well control and can be corroborative in areas with abundant well information.

9. Velocity information garnered from field reflection records in the southern Valley and Ridge has been inadequate to migrate the data in this structurally complex area. Laboratory velocity information can be used to perform geometry-dependent migrations of the records.

10. Evaluating the possibility that Valley and Ridge sedimentary rocks extend beneath the crystalline Appalachian overthrust will require high-quality seismic reflection data across the Blue Ridge front. Accurate interpretation of these data demands a thorough understanding of facies changes and the effects of progressive metamorphism on sedimentary rock velocities.

ACKNOWLEDGMENTS

The assistance of C. Wilcox, W. Wepfer, B. Plaskon, and D. Kingma in the laboratory measurements is appreciated. R. D. Hatcher, Jr. suggested the Thorn Hill section for sample collecting. H. Benz calculated the synthetic of Figure 11, and R. Smith provided computer facilities at the University of Utah for the calculation. Laboratory studies were supported by the Office of Naval Research contract N00014-89-J-1209.

REFERENCES CITED

Birch, F., 1960, The velocity of compressional waves in rocks to 10 kilobars: Journal of Geophysical Research, v. 65, p. 1083–1102.

Bryant, B., and Reed, J. C., Jr., 1970, Geology of the Grandfather Mountain window and vicinity, North Carolina and Tennessee: U.S. Geological Survey Professional Paper 615, 190 p.

Christensen, N. I., 1965, Compressional wave velocities in metamorphic rocks at pressures to 10 kilobars: Journal of Geophysical Research, v. 70, p. 6147–6164.

——— 1985, Measurements of dynamic properties of rock at elevated temperatures and presssures, *in* Pincus, H. J., and Hoskins, E. R., eds., Measurement of rock properties at elevated pressures: Philadelphia, American Society for Testing and Materials, p. 93–107.

Christensen, N. I., and Fountain, D. M., 1975, Constitution of the lower continental crust based on experimental studies of seismic velocities in granulite: Geological Society of America Bulletin, v. 86, p. 227–236.

Clark, H. B., Costain, J. K., and Glover, L., III, 1978, Structural and seismic reflection studies of the Brevard ductile deformation zone near Rosman, North Carolina: American Journal of Science, v. 278, p. 419–441.

Cook, F. A., Albaugh, D. S., Brown, L. D., Kaufman, S., Oliver, J. E., and Hatcher, R. D., Jr., 1979, Thin-skinned tectonics in the crystalline southern Appalachians; COCORP seismic-reflection profiling of the Blue Ridge and Piedmont: Geology, v. 7, p. 563–567.

Cook, F. A., Brown, L. D., Kaufman, S., and Oliver, J. E., 1983, The COCORP seismic reflection traverse across the Southern Appalachians: American Association of Petroleum Geologists Studies in Geology No. 14: Tulsa, Oklahoma, American Association of Petroleum Geologists, 61 p.

Coruh, C., Costain, J. K., Hatcher, R. D., Jr., Pratt, T. L., Williams, R. I., and Phinney, R. A., 1987, Results from regional vibroseis profiling: Appalachian ultradeep core hole site study: Royal Astronomical Society Geophysical Journal, v. 89, p. 147–156.

Harris, L. D., 1970, Details of thin-skinned tectonics in parts of Valley and Ridge and Cumberland Plateau provinces of the southern Appalachians, *in* Fisher, G. W., Pettijohn, F. J., Reed, J. C., Jr., and Weaver, K. N., eds., Studies of Appalachian geology—Central and southern: New York, Wiley-Interscience, p. 161–173.

——— 1976, Thin-skinned tectonics and potential hydrocarbon traps—Illustrated by a seismic profile in the Valley and Ridge province of Tennessee: U.S. Geological Survey Journal of Research, v. 4, p. 379–386.

Harris, L. D., Harris, A. G., DeWitt, W., Jr., and Bayer, K. G., 1981, Evaluation of southern eastern overthrust belt beneath Blue Ridge–Piedmont thrust: American Association of Petroleum Geologists Bulletin, v. 65, p. 2497–2505.

Hatcher, R. D., Jr., 1971, Stratigraphic, petrologic, and structural evidence favoring a thrust solution to the Brevard problem: American Journal of Science, v. 270, p. 177–202.

——— 1972, Developmental model for the southern Appalachians: Geological Society of America Bulletin, v. 83, p. 2735–2760.

——— 1982, Hydrocarbon resources of the eastern overthrust belt: A realistic evaluation: Science, v. 216, p. 980–982.

Hatcher, R. D., Jr., Costain, J. K., Coruh, C., Phinney, R. A., and Williams, R. T., 1987, Tectonic implications of new Appalachian ultradeep core hole (ADCOH) seismic reflection data from the crystalline southern Appalachians: Royal Astronomical Society Geophysical Journal, v. 89, p. 157–162.

Milici, R. C., Harris, L. D., and Statler, A. T., 1979, An interpretation of seismic cross sections in the Valley and Ridge of eastern Tennessee: Tennessee Division of Geology Oil and Gas Seismic Investigation Series 1.

Miller, R. L., 1973, Structural setting of hydrocarbon accumulations in folded southern Appalachians: American Association of Petroleum Geologists Bulletin, v. 57, p. 2419–2427.

Mitra, S., 1988, Three-dimensional geometry and kinematic evolution of the Pine Mountain thrust system, southern Appalachians: Geological Society of America Bulletin, v. 100, p. 72–95.

Tegland, E. T., 1978, Seismic investigations in eastern Tennessee: Tennessee Division of Geology Bulletin 78, 68 p.

Walker, K. R., ed., 1985, The geologic history of the Thorn Hill Paleozoic section (Cambrian-Mississippian) eastern Tennessee: Tennessee University Department of Geological Sciences Studies in Geology 10: Knoxville, Tennessee, Tennessee University, 128 p.

Wyllie, M.R.J., Gregory, A. R., and Gardner, L. W., 1956, Elastic wave velocities in heterogeneous and porous media: Geophysics, v. 21, p. 41–70.

Manuscript Received by the Society August 30, 1989
Revised Manuscript Received June 20, 1990
Manuscript Accepted July 6, 1990